DR ROGER D CONE (Orcid ID : 0000-0003-3333-5651)

Article type : Original Article

Obesity-associated mutant MC4 receptors with normal $G\alpha_s$ coupling frequently exhibit other discoverable pharmacological and biochemical defects

Taneisha Gillyard[1], Katelyn Fowler[2], Savannah Y. Williams[2], and Roger D. Cone[2,3]

[1]Department of Neuroscience and Pharmacology, Meharry Medical College, Nashville, TN 37208-3501, [2]Life Sciences Institute, University of Michigan, Ann Arbor, MI 48109, and [3]Department of Molecular and Integrative Physiology, School of Medicine, University of Michigan, Ann Arbor, MI 48109

Correspondence to: Roger Cone
rcone@umich.edu
734-615-9787

This is the author manuscript accepted for publication and has undergone full peer review but has not been through the copyediting, typesetting, pagination and proofreading process, which may lead to differences between this version and the Version of Record. Please cite this article as doi: 10.1111/JNE.12795

ABSTRACT

Mutations in the melanocortin-4 receptor (MC4R) are the most common cause of early syndromic obesity known. Most of these mutations result in a loss of protein expression, α-melanocyte-stimulating hormone (α-MSH) binding, receptor trafficking, or coupling to the stimulatory G-protein, $G\alpha_s$. However, approximately 26% of the obesity-associated mutations characterized to date exhibit none of these pharmacological defects. Here, we have studied 7 of these apparently normal mutant MC4R in more detail, and found that the majority (5 of the 7) exhibit marked defects including defective binding of another endogenous melanocortin ligand (β-MSH), defective glycosylation, and defective recruitment of β-arrestin. These data provide support for two hypotheses: 1) that the majority of these rare, obesity-associated mutations are likely defective and causative of obesity, and 2) that β-arrestin recruitment is a valuable marker of normal MC4R function. Recent work has demonstrated a statistical correlation between the efficacy of β-arrestin recruitment to the MC4R and BMI, however the data shown here demonstrates both decreased and increased β-arrestin signaling in obesity-associated MC4R mutations.

1 | INTRODUCTION

The central melanocortin system is known to play a pivotal role in the regulation of energy metabolism and food intake. Mutations in the central melanocortin-4 receptor (MC4R) are found in 1 out of every 1500 individuals, and are associated with up to 6% of cases of severe early-onset monogenic obesity[1,2]. MC4R is a Class A (Rhodopsin-like), seven-transmembrane G-protein-coupled-receptor (GPCR) that is shown to signal primarily through the $G\alpha_s$ -> adenylyl cyclase -> cAMP pathway. This signaling pathway in MC4R neurons is known to be required for control of thermogenesis, energy balance, and glucose metabolism[3]. A classification system was previously proposed[4] sorting obesity-associated MC4R mutations into functional classes described as loss-of-function mutations caused by defective expression (class I mutants), disrupted trafficking of the receptor (class II mutants), decreased binding affinity (class III

mutants), or defective coupling to $G\alpha_s$ (class IV mutants)[5–9]. Yet, up to 26% of obesity-associated MC4R mutations[10] exhibit normal receptor activity with respect to these four criteria[11,12]. Although it is possible that these "class V" mutations are non-pathogenic, recent studies have suggested that MC4R signaling is quite complex. The MC4R signaling complex appears to involve a number of accessory proteins[13–19]. Furthermore, the MC4R appears to signal differently in different neuronal cell types, coupling to a K_{ATP} channel to hyperpolarize cells in the brainstem[20] while coupling to an inwardly-rectifying potassium channel, Kir7.1, independent of G-proteins, mediating α-MSH-induced membrane depolarization in the paraventricular nucleus of the hypothalamus (PVN)[15,21] . The Melanocortin-2 Receptor Associated Protein 2 (MRAP2) has also been shown to suppress the constitutive activity at the receptor and regulate sensitivity to α-MSH. Deletion of MRAP2 in both zebrafish and mice has resulted in increased adiposity[13,14]. Four potentially pathogenic variants of MRAP2 were also identified in early-onset obese humans[13]. Upon ligand activation, GPCRs are known to recruit β-arrestin and were thought to only lead to receptor desensitization, internalization and either recycling of the receptor back to the membrane or downstream degradation[22]. However, recent studies have shown that recruitment of β-arrestin can couple the receptor to intracellular, G-protein independent signalling cascades[23,24]. A recent publication has demonstrated highly variable recruitment of β-arrestin by naturally occurring MC4R variants identified in the UK Biobank, and demonstrated a statistical correlation between the efficacy of β-arrestin recruitment to the MC4R and BMI[25].

Beyond simply elucidating the signalling mechanism(s) of a receptor critical to energy homeostasis, further study of this receptor is needed to advance attempts to develop small molecule therapeutics at this receptor, given the finding of a target-mediated pressor response[26–28]. A more detailed pharmacological model of receptor signalling may, for example, allow for the development of biased agonists that stimulate weight loss but not the pressor response. In order to better understand essential functional features of the MC4R that have not yet been elucidated, we have sought to identify potential biochemical and/or pharmacological defects in class V obesity-associated MC4R mutations reported to have normal cell surface expression, ligand binding, and coupling to $G\alpha_s$.

2 | MATERIALS AND METHODS

2.1 | Selection of MC4R variants

The seven MC4R variants chosen for study, Aspartate-37-Valine (D37V)[5], Proline-48-Serine (P48S)[5], Valine-50-Methionine (V50M)[5,29] , Histidine-76-Arginine (H76R)[2,11] , Isoleucine-170-Valine (I170V)[5,29], Asparagine-274-Serine (N274S)[5], and Arginine-305-Serine (R305S)[2,11] were identified from the published literature using the following criteria: (1) implicated in the development of obesity in humans, (2) resulted in a full-length protein upon translation, (3) no known molecular defects in terms of G-protein coupling, cell surface expression, and ligand binding affinity.

2.2 | Cells, plasmids, mutagenesis and transfection

All experiments were performed in Chinese Hamster Ovary (CHO-K1) cells (ATCC CC61) maintained in a 37°C tissue culture incubator with 5% CO_2. Growth media consisted of Gibco Dulbecco's Modified Eagle Medium (DMEM)/F-12 with 4-(2-hydroxyethyl)-1-piperazineethanesulfonic acid (HEPES), 10% fetal bovine serum (FBS), and 1% antibiotic/antimycotic (Anti-Anti). Cells were no longer used for experimental purposes past passage number 15. The human MC4R plasmid was obtained from cDNA.org (cat. no. MCR040TN00) and contained an N-terminal 3-human influenza hemaglutinin (3HA) tag cloned in pcDNA3.1$^+$ (from Invitrogen) with MC4R sequence cloned at KpnI and XhoI restriction sites. This plasmid was used as the template to create mutant receptor vectors via site directed mutagenesis. pSF-CMV-NEO-COOH-3xFLAG plasmid was obtained from Sigma-Aldrich (cat. no. OGS629-5UG). The sequence for wild-type human MRAP2 was cloned into SacI and XhoI restriction sites using Polymerase Chain Reaction and Quick Ligase (New England Biolabs, cat. no. M2200). All transfections were performed transiently with FuGene HD (Promega, cat. no. E2312) using a reverse transfection protocol. A cAMP-sensitive luciferase plasmid (pGL4.29), used for cAMP accumulation assays, was purchased from Promega (cat. no E8471). Plasmids for the NanoBit assay (Promega N2014) were provided in the starter kit (Promega, cat. no N2014). Human β-arrestin 2 coding sequence was cloned into C-terminal SmallBit plasmid at EcoRI and SacI restriction sites. Cloning of mutant human MC4R receptors into N-terminal LargeBit was performed by amplifying mutant MC4R sequence via PCR using corresponding oligonucleotide primers, followed by Dpn1 digestion, restriction enzyme digestion, dephosphorylation of open vector, quick ligation, and E. coli transformation.

2.3 | Antibodies

Western blotting was performed using the following antibodies: HA-tag (6E2) Mouse (Cell Signaling Technology, cat. no. 2999); HA-tag (6E2) Mouse mAb (HRP Conjugate) (Cell Signaling Technology, cat. no. 2367) diluted 1:5,000 ; Anti-FLAG M2 Mouse (Sigma-Aldrich, cat. no. F3165); Anti-FLAG M2-Peroxidase Mouse (Sigma-Aldrich, cat. no. A8592) diluted 1:10,000; GAPDH (D16H11) XP Rabbit (HRP Conjugate) (Cell Signaling Technology, cat. no. 8884S) diluted 1:5,000; Beta-actin (8H10D10) mouse mAb (Cell Signaling Technology, cat. no. 3700S) diluted 1:5,000; and anti-mouse IgG, HRP-linked (Cell Signaling Technology, cat. no. 7076S) diluted 1:10,000

2.4 | In vitro mutagenesis of MC4R

Mutant MC4R receptors were created via site-directed mutagenesis using QuikChange II XL (Agilent, cat. no 200521) and provided protocol. Following PCR amplification, plasmids were transformed into provided ultracompetent XL-10 gold *Escherichia coli* cells and allowed to propagate in a 37°C rocking incubator for 1 hour before streaking on a Luria broth (LB) agar plate containing ampicillin. These plates were incubated overnight at 37°C and single colonies were picked and inoculated in liquid LB media containing ampicillin and allowed to propagate overnight. DNA was then isolated from bacterial cultures using QiaPrep mini-prep kit (Qiagen, cat. no. 27106). Mutagenesis was then confirmed via Sanger sequencing provided by the DNA sequencing core at the University of Michigan (Ann Arbor, MI) prior to use in experimental assays.

2.5 | MSH-induced $G\alpha_s$ coupling and accumulation of intracellular cAMP

CHO-K1 cells were plated and transfected in white, flat-bottomed 96 well plates (Corning, cat. no. CLS3917) with a cAMP sensitive luciferase plasmid and corresponding empty vector, variant receptor, and/or MRAP2 plasmids using methods as described above. Transfection was performed with 0.2µg of DNA/well (0.1µg luciferase and 0.1µg of experimental plasmids). Variant receptor +/- MRAP2 (or empty vector) was transfected at a 1:6 ratio. Each condition was plated in triplicate. Forty-eight hours following transfection, growth media was removed and 50µl of Opti-MEM was added to each well (Gibco, cat no. 11058021).

50µl of a serial dilution (starting concentration of 10pM, ending concentration of 1µM) of α-MSH (Bachem cat. no. H-1075), β-MSH (Phoenix Pharmaceuticals, cat. no 043-12) or des-acetyl-α-MSH (Bachem, cat. no. H-4390) was then added to corresponding wells as well as a forskolin (Sigma Aldrich, cat. no F6886) control for each transfection condition. Cells were allowed to incubate at 37°C for 4 hours. Following incubation, all liquid was removed from the cells and 50µl of room temperature Dulbecco's Phosphate-Buffered Saline (DPBS) (Gibco, cat. no 14040133) was added to the cells followed by 50ul of room temperature ONE-Glo EX luciferase substrate (Promega, cat. no E8120). Plate was covered with foil and allowed to incubate at room temperature for 10 minutes on an orbital rocker before reading luminescence on an Enspire microplate reader (PerkinElmer). Averages of triplicate conditions were calculated using Excel and expressed as a percentage of the wild-type maximum response. Concentration response curves were generated by pooling data from three independent experiments. Maximal responses (E_{max}) and EC_{50} values were calculated using GraphPad Prism software. A one-way ANOVA statistical test was applied to pEC_{50} and E_{max} values to determine significance ($p<0.05$), with Bonferonni post-HOC for multiple comparisons.

2.6 | Co-immunoprecipitation

CHO-K1 cells were transiently transfected in 6cm poly-D-lysine coated plates using FuGene HD transfection reagent (Promega) and allowed to incubate at 37°C for 48 hours. DNA concentrations were as follows: 5µg of DNA was transfected per plate. Receptor variant +/- MRAP2 or empty vector was transfected at a 1:3 ratio. Cells were gently rinsed twice with room temperature DPBS followed by crosslinking for 15 minutes at room temperature with 1mM dithiobis(succinimidyl propionate) (DSP) (Thermo Scientific, cat.no PG82081). Reaction was stopped using 10mM tris(hydroxymethl)aminomethane-hydrochloride (Tris-HCL) solution for 15 minutes at room temperature. Cell lysates were then harvested by adding radioimmunoprecipitation assay buffer (RIPA buffer) to each plate followed by scraping and allowing plate to incubate on rocker at 4°C for 30 minutes. Contents of each plate were then added to a clean Eppendorf tube and centrifuged at 10,000 rpm for 10 minutes. Supernatants were collected in fresh Eppendorf tubes followed by Pierce bicinchoninic acid (BCA) protein quantification assay. 100ug of lysate in a total volume of 500µl was incubated with 1ug of antibody on a rotator at 4°C overnight. Next day, protein G magnetic beads (Thermo Scientific,

cat. no 88848) were rinsed and resuspended in RIPA buffer. 30µl of beads were added to each tube and allowed to incubate on rocker at 4°C for 1 hour. Using a magnetic rack, beads were washed three times with RIPA buffer and eluted in 50µl of 3X lithium dodecyl sulfate (LDS) buffer (Thermo Scientific, cat. no B0007) with 200mM DTT. Samples were allowed to rest at room temperature for 15 minutes before loading 20µl on sodium dodecyl sulfate-polyacrylamide gel electrophoresis (SDS-PAGE) gel. Blots were imaged on ChemiDoc (Bio-Rad).

2.7 | Endoglycosidase treatment for confirmation of MC4R glycosylation

CHO-K1 cells were plated and transfected in 10cm poly-D-lysine coated plates in the same manner as previously detailed and allowed to incubate at 37°C for 48 hours. Cells were transfected with 8µg of receptor variant DNA per plate. Cell lysates were then harvested as described above. To assess glycosylation pattern, Endo H (New England BioLabs, cat. no. P0702S) and PNGase F (New England BioLabs, cat. no. P0704S) were used following the provided protocols. Samples were then run on an SDS-PAGE gel and analyzed via western blot using ChemiDoc imager and Bio-Rad Image Lab analysis software.

2.8 | Western blots

10-15ug protein from prepared cell lysates were loaded into corresponding lanes on Invitrogen Bolt 4-12% Bis-Tris Plus precast polyacrylamide gels (Invitrogen, cat. no. NW04122) at 200V for 30-40 minutes using Bolt MOPS running buffer (Invitrogen, cat. no. B000102). Bolt antioxidant (Invitrogen, cat. no. BT0005) was added to the first chamber of the mini gel tank (Invitrogen, cat. no. A25977). Transfer to Immobilon polyvinylidene fluoride (PVDF) membrane (Millipore, cat. no. IPVH00010) was performed using transblot turbo system (Bio-Rad, cat. no 1704150EDU). Membranes were blocked with 5% non-fat dry milk in phosphate buffered saline with 1% Tween-20 overnight at 4°C. Blots were then washed a minimum of three times for 15 minutes each before imaging using SuperSignal West Dura Extended Detection Substrate (ThermoScientific, cat. no. 34075) using the BioRad ChemiDoc Touch Imaging System.

2.9 | MSH-induced β-arrestin recruitment

CHO-K1 cells were transiently transfected in white, flat-bottomed 96 well plates with wild-type or mutant-MC4R-LgBit and SmBit-β-arrestin plasmids (0.2ug of DNA/well at 1:1 ratio) using FuGene HD transfection reagent and allowed to incubate at 37°C for 48 hours. On the day of experiment, all media was removed from cells and replaced with 25µl of room temperature DPBS (Gibco) and allowed to equilibrate at room temperature for 10 minutes. 25ul of room temperature NanoGlo Live Cell Substrate was then added to each well, the plate was wrapped in foil, and gently mixed on an orbital shaker for 15 seconds. Background luminescent signal was measured for 5 minutes using the PerkinElmer Enspire microplate reader. 50µl of a serial dilution (starting concentration of 10pM, ending concentration of 10µM) of α-MSH or β-MSH was added to corresponding wells, covered with foil, and allowed to incubate at room temperature for 10 minutes before measuring luminescent signal on microplate reader. 10 minutes was chosen as an optimal time point, since signal was observed to peak at this time. Each condition was measured from triplicate wells in each experiment, and each experiment was performed at least three times independently. For data analysis, raw values for background measurement were averaged and used to normalize MSH response for each corresponding well. The normalized values for the stimulated wells were then averaged. Concentration response curves were generated by pooling data from three independent experiments. The concentration response curves for these data were generated in GraphPad Prism and analyzed to determine E_{max} and EC_{50}. A one-way ANOVA statistical test was applied to pEC_{50} and E_{max} values to determine significance ($p<0.05$), with Bonferonni post-HOC for multiple comparisons.

3 | RESULTS

3.1 | $G\alpha_s$-coupling of MC4R variants in response to α- and β-MSH

In this study, 7 different human obesity-associated class V variants of the MC4R (Figure 1) were characterized in CHO-K1 cells. These seven mutations were previously identified in obese patients and assessed for G-protein coupling, binding affinity, and cell surface expression[30] and categorized as Class V variants, based on normal cell surface expression, ligand binding, and coupling to $G\alpha_s$[30].

To characterize the coupling of the mutant receptors to $G\alpha_s$ in response to α-MSH or β-MSH, we used a cAMP-responsive luciferase to measure the accumulation of cAMP upon activation by either ligand. In response to α-MSH (Figure 2A-F), one variant (V50M) exhibited

a significant increase in EC_{50}, while two variants (V50M, H76R) exhibited a significant decrease in E_{max}. In response to β-MSH (Figure 2G-L), one variant exhibited a significant increase in EC_{50} (H76R), while I170V exhibited an increase in maximum response. These data suggest that five of these receptor variants exhibit fully normal responses to both α-MSH and β-MSH (D37V, P48S, I170V, N274S, R305S; Table 1). H76R also exhibited significant constitutive activity in our assay (Supplemental Figure 1).

A recent study found that des-acetyl-α-MSH was the predominant form of MSH in the adult human brain[31]. Previous studies in which α-MSH was used to perform molecular assays used acetylated α-MSH, which was also used in these experiments. To verify whether or not the acetylation status of MSH might have affected these results, we ran the cAMP accumulation assay and compared findings using WT and 2 variant receptors (D37V and V50M); Supplemental Figure 2). No significant differences were found when comparing EC_{50} values in response to α-MSH versus des-acetyl-α-MSH at the WT and variant receptors tested.

3.2 | MRAP2 interacts with and is able to suppress constitutive activity of all variants

In this study, we sought to test the hypothesis that class V obesity-associated MC4R receptors associated with obesity have defects in signaling not detected by a conventional $G\alpha_s$ coupling assay. MC4R exhibits a significant degree of constitutive activity, and MRAP2 has been shown to inhibit this activity, as well as increase responsiveness to α-MSH[14]. Thus, mutations enhancing the suppression of MC4R activity by MRAP2, or compromising MRAP2 effects on responsiveness to ligand, might be expected to reduce MC4R activity, which could be expected to cause obesity. To characterize the protein-protein interaction between MRAP2 and MC4R variants, we first performed co-immunoprecipitation from cell lysates collected from CHO-K1 cells that were transiently transfected with WT or mutant MC4R (N-terminal 3HA epitope tag; anticipated MW: 37 kDa) with or without co-transfection of MRAP2 (C-terminal 3xFLAG epitope tag; anticipated MW: 28 kDa). According to previous studies, MRAP2 pulls down as a doublet representing unglycosylated and glycosylated forms of the protein. The band observed above this doublet has been suggested to be a more highly glycosylated form of MRAP2, however, this is yet to be confirmed. We found that each MC4R variant was able to pull down MRAP2 in a manner comparable to wild-type MC4R (Figure 3A).

To assess the ability of MRAP2 to suppress the constitutive activity of each variant, we performed a luciferase-based assay measuring the basal levels of cAMP in CHO-K1 cells transiently transfected with WT or mutant MC4R with or without MRAP2 (Figure 3 B). We further tested whether MRAP2 had any effect on the WT or mutant receptor's response to α-MSH or β-MSH and found that there no significant differences (Supplemental Figure 3). Together, these results show that there were no defects in these class V variants in suppression of constitutive activity, or alteration in ligand responsiveness by MRAP2.

3.3 | V50M variant exhibits a putative defect in N-linked glycosylation

We next examined the glycosylation state of each variant MC4R protein. Using cell lysates from transiently transfected CHO-K1 cells, we performed western blots to assess the size and banding pattern of the WT and mutant MC4Rs. Interestingly, MC4R V50M exhibited an altered migration pattern compared to WT and this pattern was similar to a variant of MC4R (N26Q) in which one of four N-linked glycosylation sites had been mutated (Figure 4A). We used the Endo H and PNGase F endoglycosidases to confirm the glycosylation of WT MC4R and verify the defect in receptor glycosylation by the V50M mutation. PNGase F is able to cleave all glycans, core and complex, from a protein while the Endo H enzyme is only able to cleave core glycans. Therefore, if a protein has complex glycosylation, it will be resistant to Endo H, but not PNGase F, and there will be no band shift observed. Results from these experiments (Figure 4B) suggest that WT MC4R undergoes core but not complex glycosylation. V50M again exhibits an altered migration pattern compared to WT MC4R and similar to the N26Q mutant. Both of these mutations are shown to be glycosylated, but not to the same extent as WT, thus, absence of a single glycosylation event in the V50M mutant is consistent with the data.

3.4 | Five of seven variants tested have altered β-arrestin recruitment in response to α- or β-MSH

Upon activation, GPCRs are known to recruit β-arrestin, which leads to downstream intracellular events such as receptor internalization, or to novel pathways of intracellular signaling. To assess the recruitment of β-arrestin to WT and mutant MC4Rs in response to α-MSH or β-MSH, we utilized the NanoBit luciferase-based complementation assay (Promega).

WT or mutant receptors were fused to the "large bit" of a Nano-luciferase enzyme at the C-terminal end while β-arrestin was fused to the "small bit" at the N-terminal end. These constructs were then transiently co-transfected into CHO-K1 cells and treated with α-MSH or β-MSH. To assess whether the fusion of the "large bit" affects the "normal" signaling of the receptor, we compared the 3HA-WT-MC4R construct to the LgBit-fused receptor at coupling to Gs via the cAMP accumulation assay described previously. We found that the fusion of the "large bit" did suppress the constitutive activity of the receptor and altered the EC_{50} values, compared to the un-fused receptor but did not affect its ability to respond normally to ligand. (Supplemental Figure 4A-D). To verify that MC4R-arrestin interaction was specific, we co-transfected CHO-K1 cells with HaloTag protein fused to the "small bit" (Promega), and MC4R wt and mutant constructs, fused to large bit. The HaloTag protein is expressed throughout the cell and should not interact with "large bit" fused proteins in a concentration-dependent manner. We found this to be true in our experimental set-up (Supplemental Figure 4E-H), therefore suggesting that the β-arrestin recruitment, and any observed defects, are specific to ligand-induced MC4R activation. Five of the seven variants tested had either reduced or excessive β-arrestin recruitment in response to α-MSH or β-MSH (Figure 5
and Table 1). P48S, V50M, H76R, I170V, and N274S had either or both altered EC_{50} or E_{max} for β-arrestin recruitment compared to WT in response to α-MSH, while P48S, V50M and H76R had either or both altered EC_{50} or E_{max} compared to WT in response to β-MSH. These data suggest that the interaction between MC4R and β-arrestin is an important pathway in the regulation of MC4R signaling and its normal function in maintaining body weight.

4 | DISCUSSION

The melanocortin-4 receptor is one of the most well-validated drug targets for the treatment of obesity. However, many peptide and small molecule drugs targeting MC4R have failed in clinical trials due to a target-mediated increase in blood pressure[26–28]. The growing interest in biased signaling in GPCR drug discovery highlights the urgency to explore novel signaling pathways when thinking of target-specific therapeutics[32–36]. Interestingly, there are a subset of MC4R mutations found in humans that are associated with the development of obesity, yet have been reported to couple normally to $G\alpha_s$. It has been shown that upon MC4R agonist binding, $G\alpha_s$-signaling leads to activation of adenylyl cyclase and elevation of intracellular

cAMP that may go on to activate cAMP responsive element-binding protein (CREB)[37]. Some data suggests that $G\alpha_s$ signaling is critical for MC4R signaling and regulation of body weight, since deletion of the GNAS gene encoding $G\alpha_s$ in MC4R neurons recapitulates the entirety of the obesity syndrome following MC4R deletion[3,38]. However, deletion of CREB in the PVN has no influence on the ability of MC4R agonist, MTII, to inhibit food intake[39]. These data, along with the complexity of MC4R signaling and multiple MC4R accessory proteins further highlight the likelihood that multiple signaling pathways are important for the function of MC4R and its regulation of food intake and body weight. Being able to identify receptor variants with specific pathway defects would allow further insight into the complexity of MC4R-mediated regulation of energy homeostasis and potentially aid in the development of therapeutics for the treatment of obesity without the side effect profile. Erk1/2 activation is known to occur downstream of both G protein and β-arrestin signaling, thus in a previous study, only a small fraction of class V mutants tested (5 of 25) exhibited reduced Erk1/2 phosphorylation following NDP-α-MSH treatment of 293 cells transfected with MC4R[40].

In this study, we functionally characterized 7 class V variants of the MC4R and showed that there are indeed other G-protein dependent and independent signaling pathways that are defective in most of the receptor mutants in this class (Table 2). Mutations in the region of the POMC gene that encodes β-MSH has been shown to result in severe obesity in humans, providing evidence that it is also an important ligand in the central control of energy homeostasis[40–42]. We show here that some class V mutants, such as H76R, exhibit reduced responsiveness to β-MSH in both $G\alpha_s$ coupling and β-arrestin recruitment assays. This further supports the hypothesis that loss of β-MSH activity at MC4R is important for the normal regulation of energy homeostasis.

The most surprising finding was that a majority of the obesity variants characterized in this study exhibited alteration in β-arrestin recruitment. While this manuscript was in preparation, a study of a large collection (49) of naturally occurring variants of the MC4R demonstrated a statistical correlation between the efficacy of β-arrestin recruitment to the MC4R and BMI; a correlation not found with coupling to Gαs[25]. Importantly, many of these variants analysed in this study are not associated with morbid syndromic obesity. In contrast, the majority of obesity-associated mutations result in defective cAMP signalling. Further, while 4 of 7 obesity-associated mutations characterized here exhibited decreased β-arrestin recruitment, 1

exhibited an increase in maximal β-arrestin recruitment (P48S), while a second indicated a trend towards increased β-arrestin recruitment (D37V). In these cases, it is possible that the mutations lead to obesity by increasing internalization, rather than producing defective β-arrestin signal transduction.

Thus, distinct from the argument in Lotta et al. [25], our interpretation of the data suggests that β-arrestin recruitment is a marker of normal MC4R function, but that the data do not yet support a role for β-arrestin signaling in BMI. While Lotta et al. did not report the EC_{50} values for β-arrestin recruitment, it is important to note from the data presented here that, while EC_{50} values are highly assay dependent, we nonetheless observed that the native ligand α-MSH is more than two hundred fold more potent in $G\alpha_s$-mediated signalling than recruitment of β-arrestin, with fusion of the large bit tag (Supplemental Figure 4) only accounting for a 10-fold shift in EC50 (EC_{50} for α-MSH induced coupling to $G\alpha_s = 3.4x10^{-10}$; EC_{50} for α-MSH induced β-arrestin recruitment = $8x10^{-8}$). Further experimentation is necessary to identify the molecular and physiological consequences of β-arrestin recruitment to the MC4R, since MC4R signaling through β-arrestin has not yet been demonstrated.

Previous studies have shown that MC4R exhibits constitutive activity and that this is linked to the N-terminal domain of the receptor[45]. A cluster in the N-terminal domain of the receptor was identified after characterization of several naturally occurring, obesity-associated mutations of the MC4R. None of the receptor variants that were included in this study are located in this cluster, however, constitutive activity has also been shown to be regulated by interaction with the accessory protein, MRAP2[14,43]. We show here that co-expression of the MRAP2 *in vitro* is still able to suppress the constitutive activity of the 7 class V receptors tested here. Expansion of the variants tested could possibly lead to the identification of variants with defects in MRAP2 interaction. The possibility of MC4R coupling to other G-proteins is still up for debate. It is noted that some studies have claimed that MC4R interacts with the inhibitory G-protein, $G_{i/o}$, which leads to a decrease in cAMP production[44]. Other studies suggest MC4R couples to $G_{q/11}$ and mediates the mobilization of intracellular free calcium[45,46]. However, we did not include these experiments in our study because coupling to these pathways is not a reliable readout in an overexpression system and is highly variable between cell lines.

It is possible that other pathways that have not been tested here could be affected, such as other posttranslational modifications (e.g. phosphorylation, palmitoylation, etc.), receptor dimerization or interaction with other membrane proteins and/or channels (e.g. Kir7.1). Asn-linked glycosylation was shown to be significant in the function of Rhodopsin, another class A GPCR[50]. MC4R has four glycosylation sites but the function of this receptor modification is still unclear. One of the variants tested here, V50M, did exhibit a defect in glycosylation, reduced responsiveness to α- and β-MSH, and reduced ability to couple to β-arrestin, but it is unclear if the glycosylation defect contributes to the altered signaling properties. Granell et al[47] suggest that glycosylation status may not affect the function of the receptor.

In conclusion, through careful analysis of pharmacological properties, we demonstrate here that 5 of 7 class V receptors tested have marked functional defects detectable in a simple transfection cell system. It is possible that some mutations, such as the D37V or R305S mutations for which we found no significant phenotypes, are not causally linked to obesity, have defects that are only detectable in a neuronal cell milieu, or are defective in yet unknown pharmacological properties of the receptor. A second conclusion from this study is that a majority of class V MC4R mutations associated with obesity exhibit either decreased or increased β-arrestin recruitment. This finding suggests that MC4R must couple normally to β-arrestin for the normal regulation of energy homeostasis, and that biased ligands, differentiating β-arrestin from $G_s\alpha$ signaling, should be developed and tested to determine the physiological consequences of β-arrestin recruitment to the MC4R.

ACKNOWLEDGEMENTS

This study was supported by NIH RO1 DK070332 (RDC) and F31 DK107253 (TG). We thank Savannah Y. Williams for her technical assistance, Sheridan J. Carrington for his insight on the endoglycosidase assay, Alys Peisley for providing the MRAP2-3XFLAG construct and Luis Gimenez for his assistance with cloning of the NanoBit assay constructs.

REFERENCES

1. Farooqi, I. S. *et al.* Clinical Spectrum of Obesity and Mutations in the Melanocortin 4 Receptor Gene. *N. Engl. J. Med.* **348,** 1085–1095 (2003).
2. Stutzmann, F. *et al.* Prevalence of melanocortin-4 receptor deficiency in Europeans and their age-dependent penetrance in multigenerational pedigrees. *Diabetes* **57,** 2511–8 (2008).
3. Podyma, B. *et al.* The stimulatory G protein $G_s\alpha$ is required in melanocortin 4 receptor–expressing cells for normal energy balance, thermogenesis, and glucose metabolism. *J. Biol. Chem.* **293,** 10993–11005 (2018).
4. Tao, Y.-X. Molecular mechanisms of the neural melanocortin receptor dysfunction in severe early onset obesity. *Mol. Cell. Endocrinol.* **239,** 1–14 (2005).
5. Tao, Y.-X. & Segaloff, D. L. Functional characterization of melanocortin-4 receptor mutations associated with childhood obesity. *Endocrinology* **144,** 4544–51 (2003).
6. Granell, S. *et al.* A novel melanocortin-4 receptor mutation MC4R-P272L associated with severe obesity has increased propensity to be ubiquitinated in the ER in the face of correct folding. *PLoS One* **7,** e50894 (2012).
7. MacKenzie, R. G. Obesity-associated mutations in the human melanocortin-4 receptor gene. *Peptides* **27,** 395–403 (2006).
8. Srinivasan, S. *et al.* Constitutive activity of the melanocortin-4 receptor is maintained by its N-terminal domain and plays a role in energy homeostasis in humans. *J. Clin. Invest.* **114,** 1158–1164 (2004).
9. Vaisse, C. *et al.* A frameshift mutation in human MC4R is associated with a dominant form of obesity. *Nat. Genet.* **20,** 113–114 (1998).
10. Vaisse, C. *et al.* Melanocortin-4 receptor mutations are a frequent and heterogeneous cause of morbid obesity. *J. Clin. Invest.* **106,** 253–262 (2000).
11. Wang, Z.-Q. & Tao, Y.-X. Functional studies on twenty novel naturally occurring melanocortin-4 receptor mutations. *Biochim. Biophys. Acta* **1812,** 1190–9 (2011).

12. Yeo, G. S. *et al.* A frameshift mutation in MC4R associated with dominantly inherited human obesity. *Nat. Genet.* **20,** 111–2 (1998).

13. Asai, M. *et al.* Loss of function of the melanocortin 2 receptor accessory protein 2 is associated with mammalian obesity. *Science* **341,** 275–8 (2013).

14. Sebag, J. A. *et al.* Developmental control of the melanocortin-4 receptor by MRAP2 proteins in zebrafish. *Science* **341,** 278–81 (2013).

15. Ghamari-Langroudi, M. *et al.* G-protein-independent coupling of MC4R to Kir7.1 in hypothalamic neurons. *Nature* **520,** 94–8 (2015).

16. He, L. *et al.* A biochemical function for attractin in agouti-induced pigmentation and obesity. *Nat. Genet.* **27,** 40–47 (2001).

17. LANE, P. W. & GREEN, M. C. MAHOGANY, A RECESSIVE COLOR MUTATION IN LINKAGE GROUP V OF THE MOUSE. *J. Hered.* **51,** 228–230 (1960).

18. Dinulescu, D. M. *et al.* Mahogany (mg) stimulates feeding and increases basal metabolic rate independent of its suppression of agouti. *Proc. Natl. Acad. Sci. U. S. A.* **95,** 12707–12 (1998).

19. Gunn, T. M. *et al.* The mouse mahogany locus encodes a transmembrane form of human attractin. *Nature* **398,** 152–156 (1999).

20. Sohn, J.-W. *et al.* Melanocortin 4 receptors reciprocally regulate sympathetic and parasympathetic preganglionic neurons. *Cell* **152,** 612–9 (2013).

21. Anderson, E. J. P. *et al.* Late onset obesity in mice with targeted deletion of potassium inward rectifier Kir7.1 from cells expressing the melanocortin-4 receptor. *J. Neuroendocrinol.* **31,** e12670 (2019).

22. Ferguson, S. S. *et al.* Role of beta-arrestin in mediating agonist-promoted G protein-coupled receptor internalization. *Science* **271,** 363–6 (1996).

23. Shenoy, S. K. & Lefkowitz, R. J. Seven-transmembrane receptor signaling through beta-arrestin. *Sci. STKE* **2005,** cm10 (2005).

24. Shenoy, S. K. & Lefkowitz, R. J. β-Arrestin-mediated receptor trafficking and signal

transduction. *Trends Pharmacol. Sci.* **32,** 521–33 (2011).

25. Lotta, L. A. *et al.* Human Gain-of-Function MC4R Variants Show Signaling Bias and Protect against Obesity. *Cell* **177,** 597–607.e9 (2019).

26. Greenfield, J. R. *et al.* Modulation of Blood Pressure by Central Melanocortinergic Pathways. *N. Engl. J. Med.* **360,** 44–52 (2009).

27. Fani, L. *et al.* The melanocortin-4 receptor as target for obesity treatment: a systematic review of emerging pharmacological therapeutic options. *Int. J. Obes.* **38,** 163–169 (2014).

28. Ju, S. H. *et al.* Understanding melanocortin-4 receptor control of neuronal circuits: Toward novel therapeutics for obesity syndrome. *Pharmacol. Res.* **129,** 10–19 (2018).

29. Dubern, B. *et al.* Mutational analysis of melanocortin-4 receptor, agouti-related protein, and alpha-melanocyte-stimulating hormone genes in severely obese children. *J. Pediatr.* **139,** 204–9 (2001).

30. Tao, Y.-X. The melanocortin-4 receptor: physiology, pharmacology, and pathophysiology. *Endocr. Rev.* **31,** 506–43 (2010).

31. Kirwan, P. *et al.* Quantitative mass spectrometry for human melanocortin peptides in vitro and in vivo suggests prominent roles for β-MSH and desacetyl α-MSH in energy homeostasis. *Mol. Metab.* **17,** 82–97 (2018).

32. Yang, L.-K. & Tao, Y.-X. Biased signaling at neural melanocortin receptors in regulation of energy homeostasis. *Biochim. Biophys. acta. Mol. basis Dis.* **1863,** 2486–2495 (2017).

33. Tan, L. *et al.* Biased Ligands of G Protein-Coupled Receptors (GPCRs): Structure–Functional Selectivity Relationships (SFSRs) and Therapeutic Potential. *J. Med. Chem.* **61,** 9841–9878 (2018).

34. Picard, L.-P. *et al.* Structural Insight into G Protein-Coupled Receptor Signaling Efficacy and Bias between Gs and β-Arrestin. *ACS Pharmacol. Transl. Sci.* doi:10.1021/acsptsci.9b00012 (2019)

35. Shukla, A. K. *et al.*Emerging structural insights into biased GPCR signaling. *Trends*

Biochem. Sci. **39,** 594–602 (2014).

36. Yang, Z. & Tao, Y.-X. Biased signaling initiated by agouti-related peptide through human melanocortin-3 and -4 receptors. *Biochim. Biophys. Acta*. doi:10.1016/j.bbadis.2016.05.008 (2016)

37. Glas, E. *et al.* Exchange factors directly activated by cAMP mediate melanocortin 4 receptor-induced gene expression. *Sci. Rep.* **6,** 32776 (2016).

38. Chen, M. *et al.* Gsα deficiency in the dorsomedial hypothalamus underlies obesity associated with Gsα mutations. *J. Clin. Invest.* **127,** 500–510 (2017).

39. Chiappini, F. *et al.* Lack of cAMP-response element-binding protein 1 in the hypothalamus causes obesity. *J. Biol. Chem.* **286,** 8094–105 (2011).

40. Lee, Y. S. *et al.* A POMC variant implicates beta-melanocyte-stimulating hormone in the control of human energy balance. *Cell Metab.* **3,** 135–40 (2006).

41. Millington, G. W. *et al.* Differential effects of alpha-, beta- and gamma(2)-melanocyte-stimulating hormones on hypothalamic neuronal activation and feeding in the fasted rat. *Neuroscience* **108,** 437–45 (2001).

42. Biebermann, H. *et al.* A role for beta-melanocyte-stimulating hormone in human body-weight regulation. *Cell Metab.* **3,** 141–6 (2006).

43. Bruschetta, G. *et al.* Overexpression of melanocortin 2 receptor accessory protein 2 (MRAP2) in adult paraventricular MC4R neurons regulates energy intake and expenditure. *Mol. Metab.* **18,** 79–87 (2018).

44. Büch, T. R. H. *et al.* Pertussis Toxin-sensitive Signaling of Melanocortin-4 Receptors in Hypothalamic GT1-7 Cells Defines Agouti-related Protein as a Biased Agonist. *J. Biol. Chem.* **284,** 26411–26420 (2009).

45. MOUNTJOY, K. G. *et al* Melanocortin receptor-mediated mobilization of intracellular free calcium in HEK293 cells. *Physiol. Genomics* **5,** 11–19 (2001).

46. Newman, E. A. *et al.* Activation of the Melanocortin-4 Receptor Mobilizes Intracellular Free Calcium in Immortalized Hypothalamic Neurons. *J. Surg. Res.* **132,** 201–207 (2006).

47. Granell, S. *et al.* Exposure of MC4R to agonist in the endoplasmic reticulum stabilizes an active conformation of the receptor that does not desensitize. *Proc. Natl. Acad. Sci.* **110,** E4733–E4742 (2013).

Figure Legends:

Figure 1: (**A**) Schematic representation of MC4R. Amino acids are indicated in single-letter code within circles. Those affected by mutations and assessed within this study are represented by yellow diamonds. The corresponding amino acid change is noted for each variant. N-linked glycosylation sites are represented by green squares. The seven transmembrane domains are marked by Roman Numerals. EL: extracellular loop; IL: intracellular loop. Schematic generated using Protter online interactive software (Omasits et al., Bioinformatics. 2013 Nov 21) (**B**) Wild-type like, obesity-associated mutations characterized in this study.

Figure 2: Accumulation of intracellular cAMP in CHO-K1 cells transiently transfected with WT and mutant MC4R. Transfected cells were treated with α-MSH (A-C) or β-MSH (D-F) and intracellular cAMP was measured using a luciferase-based assay described in *Materials and Methods*. All experiments were run in triplicate and performed at least three times. Concentration response curves represent the means of three independent experiments. Results are expressed as mean ± SEM. $p<0.05$(*), $p<0.01$(**), $p<0.001$(***), $p<0.0001$(****)

Figure 3: (A) MRAP2 (C-terminal 3xFLAG tag; anticipated MW: 28 kDa,) protein interaction with WT and mutant MC4Rs (N-terminal 3HA tag; anticipated MW: 37 kDa) was assessed using co-immunoprecipitation and western blot techniques described in *Materials and Methods*. Shown are single blots representative of three individual experiments per set of variants. (**B**) Effect of MRAP2 interaction on constitutive activity of WT and mutant MC4Rs was assessed using a luciferase-based assay that is described in *Materials and Methods*. Bar graphs represent the level of cAMP accumulation when CHO-K1 cells were transiently transfected with MC4R +/- MRAP2. Results are expressed as mean ± SEM of pooled data from three independent experiments.

Figure 4: (A) Cell lysates from CHO-K1 cells transiently transfected with WT or mutant MC4Rs were collected and analyzed for glycosylation pattern, seen as a shift in migration compared to WT. N26Q is a mutation of one of the known glycosylation sites of MC4R. **(B)** Confirmation of glycosylation was performed using EndoH and PNGase F glycosidases and is described in *Materials and Methods*. Boxes depict where membrane was cut.

Figure 5: Recruitment of β-arrestin in CHO-K1 cells transiently transfected with WT and mutant MC4Rs. Transfected cells were treated with α-MSH (A-C) or β-MSH (D-F) and β-arrestin recruitment was measured using a luciferase-based, enzyme complementation assay described in *Materials and Methods*. All experiments were run in triplicate and performed at least three times. Concentration response curves represent the means of three independent experiments. Results are expressed as mean ± SEM. $p<0.05$(*), $p<0.01$(**), $p<0.001$(***), $p<0.0001$(****).

Table 2. Characterization summary of variants assessed within this study

hMC4R variant	$G_s\alpha$-coupling				MRAP2 protein interaction	Effect of MRAP2 on constitutive activity	Glycosylation status	Beta-arrestin recruitment			
	α-MSH		β-MSH					α-MSH		β-MSH	
	Emax (% WT)	EC50 (nM)	Emax (% WT)	EC50 (nM)				Emax (% WT)	EC50 (nM)	Emax (% WT)	EC50 (nM)
WT											
D37V	↔	↔	↔	↔	↔	↔	↔	↔	↔	↔	↔
P48S	▲	↔	↔	↔	↔	↔	↔	▲▲	▲▲	↔	▲
V50M	▼	▲▲	↔	↔	↔	↔	Loss of single glycan	▼▼▼▼	▼▼	▼▼▼	▼▼
H76R	▼▼	↔	↔	▲▲▲▲	↔	↔	↔	▼▼▼	▼▼	▼▼▼▼	↔
I170V	↔	↔	▲	↔	↔	↔	↔	▼▼	↔	↔	↔
N274S	↔	↔	↔	↔	↔	↔	↔	↔	▼▼	↔	↔
R305S	↔	↔	↔	↔	↔	↔	↔	↔	↔	↔	↔

↔: WT-like ▲: increase (number indicates level of significance) ▼: decrease (number indicates level of significance). p<0.05(*), p<0.01(**), p<0.001(***), p<0.0001(****)

A

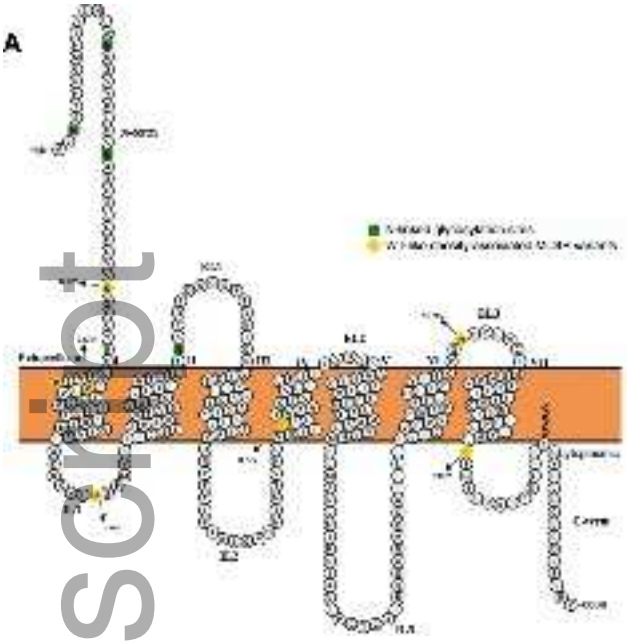

B

MC4R Variant		Topology
D37V	Asp37Val	N-term
P48S	Pro48Ser	TM-1
V50M	Val50Met	TM-1
H76R	His76Arg	IL-1
I170V	Ile170Val	TM-4
N274S	Asn240Ser	EL-3
R305S	Arg305Ser	C-term

jne_12795_f1.tiff

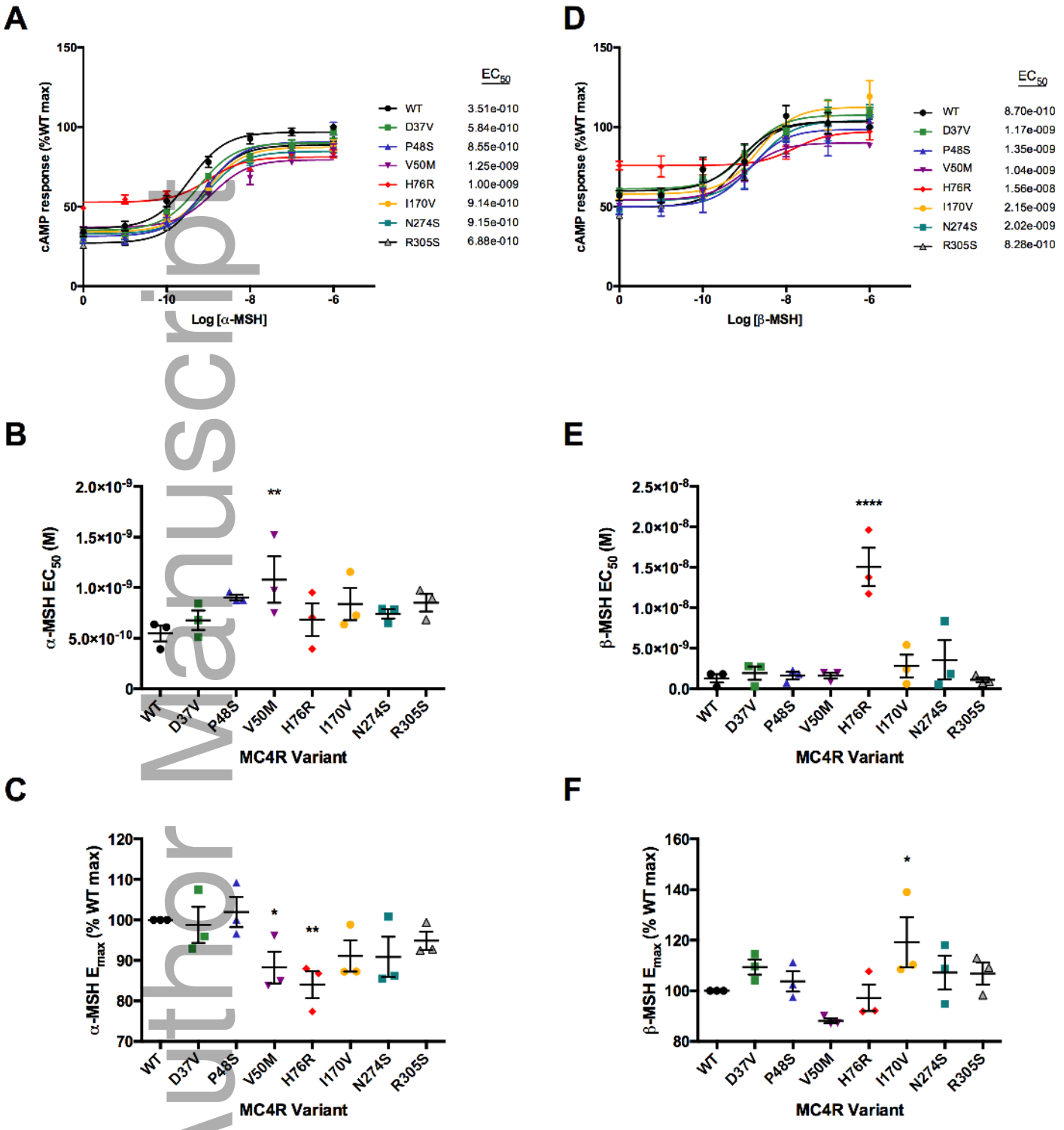

jne_12795_f2.tiff

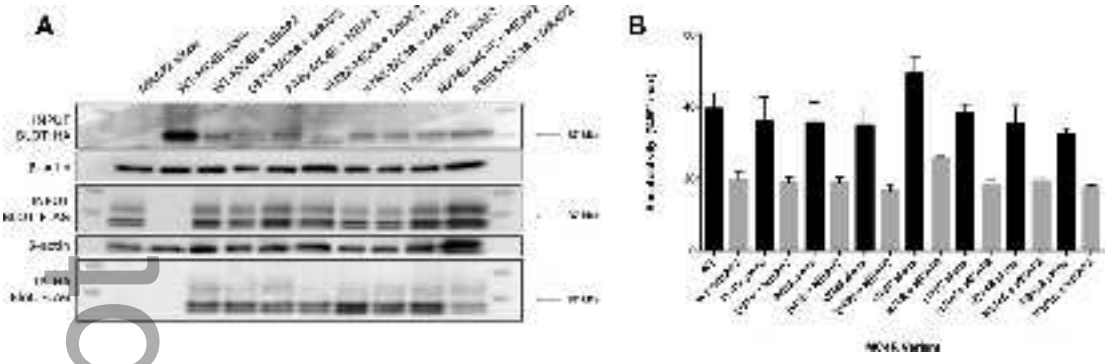

jne_12795_f3.tiff

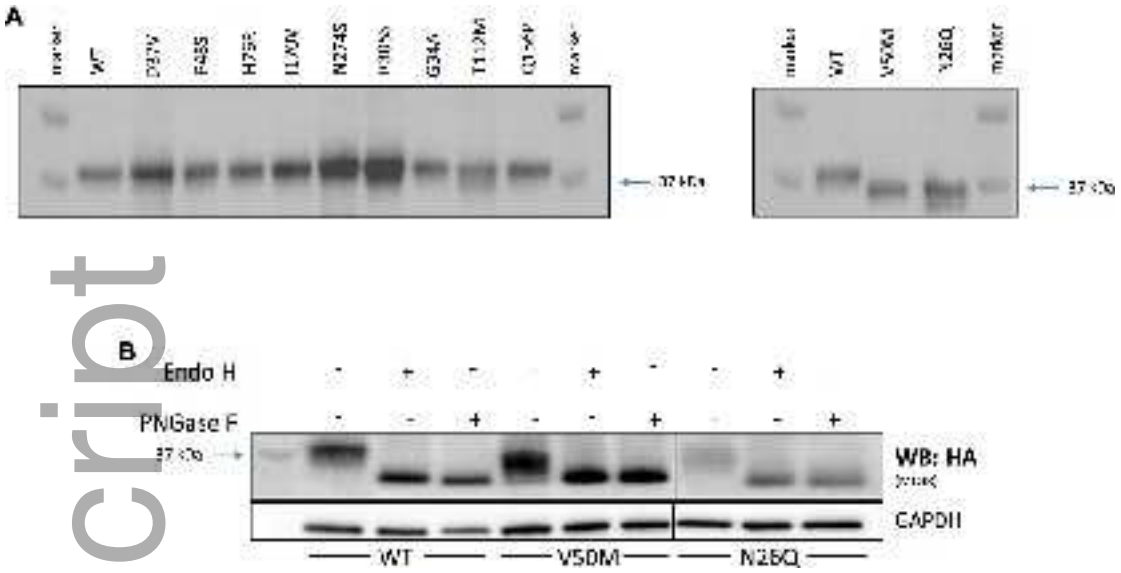

jne_12795_f4.tiff

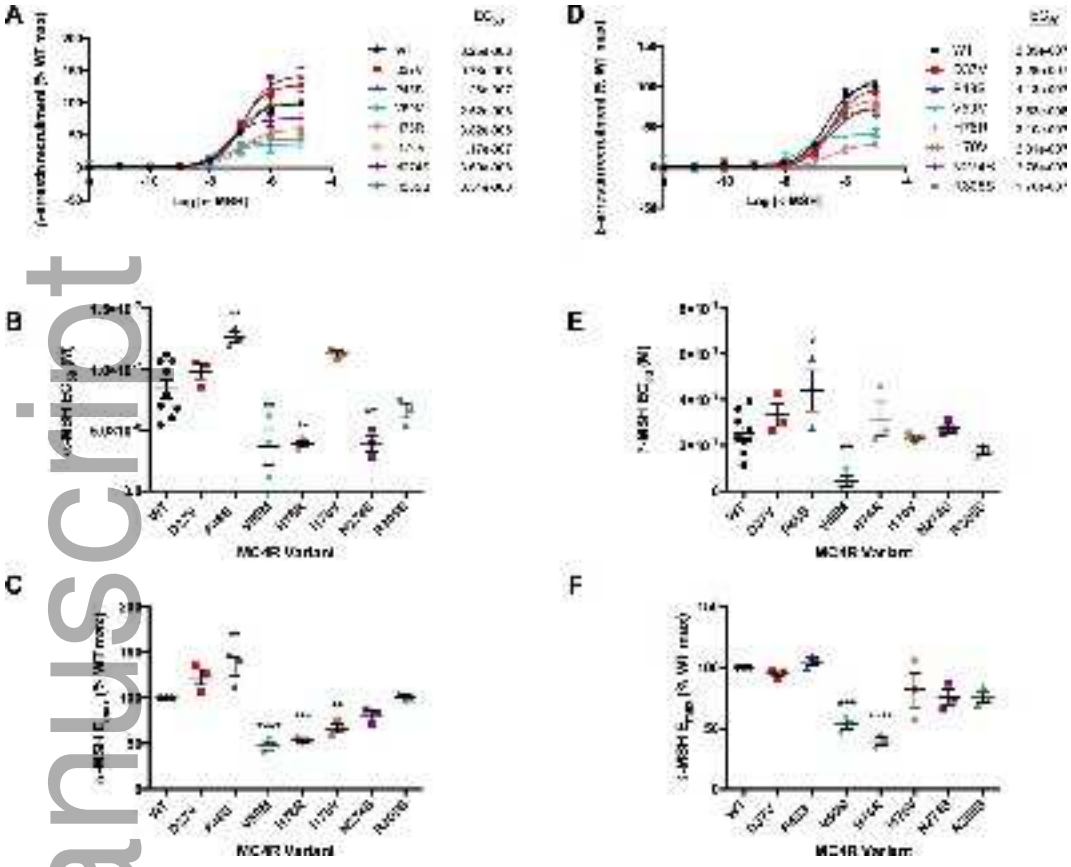

jne_12795_f5.tiff